Environmental Science and Pollution Research (2019) 26:21022–21033
https://doi.org/10.1007/s11356-019-05304-w

RESEARCH ARTICLE

# Ozonation catalyzed by iron- and/or manganese-supported granular activated carbons for the treatment of phenol

Wei Xiong[1] · Nan Chen[1] · Chuanping Feng[1] · Yang Liu[2] · Ningping Ma[2] · Jian Deng[2] · Linlin Xing[2] · Yu Gao[3]

Received: 29 December 2018 / Accepted: 26 April 2019 / Published online: 22 May 2019


## Abstract

Iron- and/or manganese-supported catalysts on granular activated carbons (Fe and/or Mn/GACs) were prepared, and their catalytic activities were evaluated by using them to treat phenol and secondary petrochemical effluent via ozonation. The presence of Fe and/or Mn/GACs significantly improved the degradation and degree of phenol mineralization. Changes in dissolved ozone concentrations and the effects of carbonate and tert-butyl alcohol (TBA) indicated that the prepared catalyst enhanced the decomposition of ozone into hydroxyl radicals (·OH), which was determined to be a key factor in catalyzing the ozonation of phenol. Typical intermediate products were identified by GC-MS and HPLC analysis, and a possible degradation pathway of phenol via catalytic ozonation was proposed. The results of XPS, CV, and other experimental data indicated that introducing Fe and/or Mn increased the rate of ozone decomposition into ·OH, and also enhanced the interfacial electron transfer by $Fe^{2+}$-$Fe^{3+}$ and $Mn^{2+}$-$Mn^{3+}$-$Mn^{4+}$ redox cycles, resulting in higher catalytic activity. However, the Fe-Mn/GAC surface was shown to undergo galvanic corrosion between $Fe_3O_4$ and $MnO_2$, decreasing the catalytic activity. In addition, catalytic ozonation was used to treat secondary petrochemical effluent. The results demonstrated that the Mn/GAC/$O_3$ system significantly improved the quality of phenol-containing wastewater in terms of its COD, TOC, $NH_4^+$-N, water color, and ecotoxicity. This study gives a better understanding of the phenol treatment by catalytic ozonation using Fe and/or Mn/GAC.

**Keywords** Phenol mineralization · Catalytic ozonation · Secondary petrochemical effluent · Redox cycle · Galvanic corrosion

**Highlights**
- Intermediate products are identified, and a phenol degradation pathway is proposed.
- Fe and/or Mn/GACs can facilitate ozone decomposition to generate ·OH.
- Catalytic performance depends on the electron transfer by $Fe^{2+}$-$Fe^{3+}$ and $Mn^{2+}$-$Mn^{3+}$-$Mn^{4+}$ redox cycles.
- Fe-Mn/GAC can undergo galvanic corrosion, decreasing its catalytic activity.
- The Mn/GAC/$O_3$ system exhibits a superior treatment performance for secondary petrochemical effluent.

Responsible editor: Vítor Pais Vilar

**Electronic supplementary material** The online version of this article (https://doi.org/10.1007/s11356-019-05304-w) contains supplementary material, which is available to authorized users.

✉ Nan Chen
chennan@cugb.edu.cn

[1] School of Water Resources and Environment, MOE Key Laboratory of Groundwater Circulation and Environmental Evolution, China University of Geosciences (Beijing), Beijing 100083, People's Republic of China

[2] Beijing BHZQ Environmental Engineering Technology, Co., LTD, Beijing 100176, People's Republic of China

[3] College of Chemical and Environmental Engineering, Shandong University of Science and Technology, Qingdao 266590, People's Republic of China

## Introduction

Water pollution by phenolic pollutants is a serious environmental problem, and has generated widespread concern because of their low biodegradability, high biotoxicity, and strong cumulative effects (Zeng et al. 2013). Several advanced oxidation technologies have been applied to remove carcinogenic and harmful organic pollutants from water and wastewater, such as Fenton processes (Wang et al. 2018), electrochemical methods (Massa et al. 2018), photocatalytic technologies (Vaiano et al. 2018), and ozone oxidation (Zhao et al. 2013).

Ozone ($O_3$) is an effective chemical oxidant (2.07 V) that can react with organic contaminants by directly oxidizing them with ozone or indirectly oxidizing them with hydroxyl radicals (·OH)(Wang and Bai 2017). Organic compounds containing unsaturated bonds or aromatic groups are particularly vulnerable to these types of oxidations (Zhu et al. 2017a). Ozonation alone is an effective oxidation process that has been used to oxidize contaminants in water and wastewater, decrease water color, control taste and odor, and kill microorganisms (Edwards-Brandt et al. 2007; Gümüş and Akbal 2017). However, $O_3$ has a low solubility and stability in water and is a highly selective oxidant, making mineralization of organic compounds by ozonation alone is more difficult (Wang and Bai 2017). In view of this, catalytic ozonation has recently emerged as a popular technology to oxidize refractory organic pollutants because of its high efficiency, low cost, and simple application (Lv et al. 2010; Li et al. 2017).

Catalytic ozonation has been developed to enhance the production of ·OH (2.8 V) for the non-selective oxidation of organic pollutants (Ma et al. 2014), thus overcoming the disadvantages of ozonation alone. Both heterogeneous and homogeneous catalytic ozonation processes have been developed for water treatment (Wu et al. 2008; Wang and Bai 2017). However, compared with the possible secondary pollution caused by metallic ions in homogeneous catalytic ozonation processes, the heterogeneous catalytic ozonation is a more promising method (Nawrocki and Kasprzyk-Hordern 2010). The most widely used materials in heterogeneous catalytic ozonation are carbon-based materials (Rivera Utrilla et al. 2011), metal oxides (Cheng et al. 2017), metal oxides attached to support materials (Afzal et al. 2016), and natural minerals (Qi et al. 2012). Unfortunately, the synthesis of most catalysts is complex and expensive, which limits their industrial applications (Chen et al. 2014a). Heterogeneous catalysts based on cheap and stable materials have been proposed to overcome these shortcomings. One prominent example is granular activated carbon (GAC), which has been used in wastewater ozonation treatments due to its low cost, abundant reserves, ease of separation and recovery, and excellent mechanical properties (Álvarez et al. 2011; Ma et al. 2016). In recent decades, many studies have been published on GAC modification using supported transition metals and their oxides, such as Mn, Fe, Cu, Co, and Ce (Chen et al. 2014a; Huang et al. 2015; Li et al. 2017). The GAC-loaded metal oxides has been reported to possess more active sites and have higher catalytic activities (Chen et al. 2014b; Tang et al. 2016).

It has been previously reported that some non-noble metal oxides with variable oxidation states and fast electron transfer abilities, such as manganese and iron oxides, have been used as active materials because of their high catalytic activities and wide availability (Liu et al. 2016; Liang et al. 2016). Iron oxides have been used in a variety of applications, including the removal of refractory organic compounds such as 2, 4, 6-trichloroanisole (Qi et al. 2012), dibutyl phthalate (Huang et al. 2015), and atrazine (Zhu et al. 2017a). Iron oxides have been reported to form ·OH by redox recycling of $Fe^{2+}$ and $Fe^{3+}$ (Bai et al. 2016). In addition, manganese oxides have also been reported to be cheap and eco-friendly catalysts for the removal of organic compounds (Faria et al. 2009), and they exhibit significant catalytic performance in the degradation of *p*-chloronitrobenzene (Cheng et al. 2017). It is generally known that manganese has variable valences states from − 3 to + 7 because of its special electronic structure (Liu et al. 2016). Therefore, the manganese oxides can easily generate mobile electrons, which would increase the formation rate of ·OH by creating a mobile-electron environment during catalytic ozonation (Lv et al. 2010; Liu et al. 2016). Since the electron mobility of manganese oxides can be further promoted by incorporating other elements (Du et al. 2018), it is therefore hypothesized that an enhanced catalytic activity could be obtained by combining iron and manganese oxides. To the best of our knowledge, few studies have focused on heterogeneous catalytic ozonation performance using Fe- and/or Mn-loaded GACs as catalysts to remove phenol and actual secondary petrochemical effluent. Furthermore, the interactions between phenol and Fe- and/or Mn-loaded GACs in ozonation processes remain unknown.

Herein, a series of Fe and/or Mn/GAC catalysts were prepared, optimized and characterized. This paper is focused on the following three aspects: (i) evaluation of the catalytic degradation performance of phenol using three types of catalysts (Fe/GAC (0.10), Mn/GAC (0.10), and Fe-Mn/GAC (0.10:0.10)); (ii) elucidation of the catalytic ozonation mechanism and the phenol degradation pathway; (iii) verification of the application of Mn/GAC in the advanced treatment of secondary petrochemical effluent.

## Experimental

### Chemicals and samples

Coconut shell granular activated carbon was purchased from Sigma-Aldrich (Sigma-Aldrich Co. Ltd., USA). Phenol (>

99.0%) and standard samples of some intermediates were obtained from Sinopharm (Sinopharm Chemical Reagent Co., Ltd., China). Other reagents such as Mn $(NO_3)_2$, Fe $(NO_3)_3 \cdot 9H_2O$, $Na_2CO_3$, and tert-butanol were of analytical grade and used without further purification. The Vibrio fischeri used for the toxicity test was obtained from the Yangtze Delta Region Institute of Tsinghua University (Zhejiang, China). Secondary petrochemical effluent was collected from Tianshi (Tianshi Energy Co. Ltd., China), and the water quality parameters were as follows: 422.5 mg $L^{-1}$ of COD, 100.0 mg $L^{-1}$ of phenol (artificial preparation), 0.011 of $BOD_5$/COD, 4.6 mg $L^{-1}$ of $NH_4^+$-N, 148.9 mg $L^{-1}$ of TOC, and solution pH of 8.3.

Fe and/or Mn/GAC catalysts were synthesized via impregnation-calcination using previously optimized conditions (Tang et al. 2016; Du et al. 2018). Initially, GAC (18–40 mesh) was washed with deionized water repeatedly and then dried at 105±1 °C for 24 h. Secondly, a fixed amount of GAC was mixed with 200 ml prepared metal salt solution (50 wt.% Mn $(NO_3)_2$, Fe $(NO_3)_3 \cdot 9H_2O$, and deionized water) in different molar concentrations at room temperature for 6 h. The mixture was then filtered, washed thoroughly with deionized water, and dried at 105±1 °C for 6 h. Finally, dried samples were calcined at 500 °C for 3 h at a heating rate of 10 °C/min, and they were then sieved for further experiments (18–40 mesh). The obtained catalysts were labeled with the molar concentration of Fe and Mn in the impregnated solution (e.g., when the molar concentration of Fe or Mn was 0.10 M, the catalysts were named Fe/GAC (0.10) and Mn/GAC (0.10)).

## Characterization of samples

To study the basic characteristics of Fe and/or Mn/GAC catalysts, the proximate characterization analyses were performed by Chinese National Standards (GB/T 212-2008). The morphologies and sizes of the catalysts were examined using a scanning electron microscopy (SEM, SSX-550, Shimadzu, Japan) at 30 kV. The chemical composition was analyzed using an energy-dispersive spectrometer (EDS, SSX-550, Shimadzu, Japan). The EDS data was randomly obtained from three different catalyst regions. The crystalline structures of samples were measured by powder X-ray diffraction (XRD, D8 Focus, Bruker, Germany), and the 2θ data from 10 to 80 was collected at 10 /min with a 0.07 step. Catalyst surface properties were measured by Fourier-transform infrared spectroscopy (FTIR, Vertex 70 V, Bruker, Germany) with a 4000–400 $cm^{-1}$ spectral range. Chemical states of the constituent elements on the catalysts were evaluated by X-ray photoelectron spectroscopy analysis (XPS, ESCALAB250Xi, Thermo Fisher, USA). Electrochemical experiments were performed on a basic electrochemical system (CHI-660B, Chinehwa, China). All experiments were conducted using a three-electrode cell configuration with a catalyst-modified conductive glass (prepared by dip-coating and drying in air at 70 ±1 °C) as the working electrode, a platinum wire as the auxiliary electrode and a saturated calomel electrode as the reference electrode. In addition, the electrolyte was a 3 wt% NaCl solution.

## Catalytic ozonation experiments

Catalytic ozonation of phenol and secondary petrochemical effluent by using Fe and/or Mn/GAC catalysts was carried out in a lab-scale reactor with an effective volume of 2.0 L (internal diameter = 8.0 cm and height = 50.0 cm). The reactor used bottom ventilation, which allowed the catalysts to mix more uniformly. A water sample (2.0 L; pH = 7.0) was added into the reactor, and then 2.0 g catalysts were introduced. Ozone generated from dried oxygen gas by a laboratory ozone generator (CF-G-3-10 g, QingDaoGuolin, China) was bubbled into the bottom of the reactor at a flow rate of 3.0 L/min by a titanium alloy porous diffuser. The ozone concentration was controlled by adjusting the electricity voltage, and the residual ozone in the off-gas was absorbed by a 20% KI solution. Ozonation experiments were terminated by bubbling a stream of $N_2$ for 5 min. Used catalysts were separated and then dried at 105±1 °C for 24 h after being washed with deionized water to prepare them for further characterization and reuse.

## Analytical methods

The concentrations of phenol and typical intermediate products were measured using high-performance liquid chromatography (HPLC, 1260 Series, Agilent, USA) with a VWD detector. The stationary phase was a mixture of acetonitrile and ultrapure water (7:3, by volume), and the injection volume was 20 μL. Intermediate products were analyzed using a gas chromatography coupled with mass spectrometry (GC-MS, 7860B/5977B Series, Agilent, USA). The injector temperature was 275 °C, and the temperature of the column oven was initially set at 70 °C for 5 min, at a ramp rate of 5 °C/min to 275 °C where it was held for 5 min. Helium was the carrier gas at a constant flow rate of 1 mL/min. Samples were extracted three times with hexane and then concentrated by purging with nitrogen gas. The concentrations of dissolved Fe and Mn in the treated wastewater during catalytic ozonation using Fe and/or Mn/GACs were analyzed by inductively coupled plasma optical emission spectrometry (ICP-OES, iCAP7000, Thermo, USA). The total organic carbon (TOC) was analyzed with a Multi TOC/TN Analyzer (2100, Analytik Jena, Germany). Ozone concentrations in the gaseous and aqueous phases were measured using the iodometric and indigo methods (Ozone Standards Committee Method), respectively. $BOD_5$, COD, and $NH_4^+$-N were analyzed according to standard examination methods

of water and wastewater (CSEPB 2002). The acute toxicity test was conducted using a microorganism fluorescence detector (AF-100, TOA-DKK, Japan) according to the standard method (UNE-EN-ISO 11348-32007) (Li et al. 2018).

## Results and discussion

### Characterization of catalysts

Catalysts were characterized using SEM, EDS, XRD, and FTIR (see Supplementary Material Test S1, Table S1, and Figs. S1-S2). As shown in Fig. S1, it is clear that Fe and Mn oxide nanoparticles were successfully and evenly coated on the surface of GACs. EDS analysis (Table S1) showed that the atomic percentage of Fe on the surfaces of Fe/GAC (0.10) and Fe-Mn/GAC (0.10:0.10) was ~ 0.90%, and that of Mn on the surfaces of Mn/GAC (0.10) and Fe-Mn/GAC (0.10:0.10) was ~ 0.30%. According to XRD analysis (Fig. S2), no diffraction Fe and Mn oxide diffraction peaks were observed on the surface of the catalysts, indicating the oxides were amorphous (Chen et al. 2017a; Li et al. 2017). FTIR spectroscopy (Fig. S3) showed a decrease in the O-H peak intensity after catalytic ozonation, demonstrating that the O-H might be partially consumed during the reaction (Bai et al. 2016). Moreover, the addition of Fe or Mn oxides did not increase the hydroxyl group density on the catalyst surfaces.

To better understand the roles of Fe and Mn oxides in a catalytic ozonation system, XPS spectra of Fe and Mn were recorded before and after catalytic ozonation of phenol. There were two main asymmetric peaks in the Fe2p spectra (Fig. 1a) at 711.0 ± 0.2 and 725.0 ± 0.2 eV which corresponded to $Fe2p_{3/2}$ and $Fe2p_{1/2}$, respectively. These positions are consistent with the iron assignments of magnetite (Tan et al. 2014; Zhu et al. 2017a), showing that $Fe^{3+}$ from magnetite was present on the catalyst surfaces. Based on the Fe2p data, $Fe^{2+}$ and $Fe^{3+}$ accounted for 62.78% and 37.22% ($Fe^{x+}/(Fe^{2+} + Fe^{3+})$) in the fresh Fe-Mn/GAC catalyst, while 70.90% and 29.10% were in the used catalyst, respectively (Table S2). This verifies that $Fe^{2+}$ and $Fe^{3+}$ participated in the redox reaction during the catalytic ozonation of phenol. The Mn2p regions of the XPS spectra (Fig. 1b) have $Mn2p_{3/2}$ binding energy peaks located at 641.35 eV, 642.80 eV, and 645.90 eV, which correspond to $Mn^{2+}$ (MnO), $Mn^{3+}$ ($Mn_2O_3$ or $Mn_3O_4$), and $Mn^{4+}$ ($MnO_2$), respectively (Umezawa and Reilley 1978; Strohmeier and Hercules 1984; Zhang et al. 2015; Liu et al. 2016; Du et al. 2018). Interestingly, as shown in Table S2, the percentages of different manganese ions ($Mn^{x+}/(Mn^{2+} + Mn^{3+} + Mn^{4+})$) showed slight changes after the catalytic ozonation of phenol (Table S2), which indicated that the transitions occurred among $Mn^{2+}$, $Mn^{3+}$, and $Mn^{4+}$ during the redox process. For example, the relative amount of $Mn^{4+}/(Mn^{2+} + Mn^{3+} + Mn^{4+})$ decreased from 23.87 to 19.85% due to the reaction between the strongly oxidizing $Mn^{4+}$ and organic compounds (Li et al. 2015). As previously reported (Lv et al. 2010; Bai et al. 2016), $Fe^{2+}$-$Fe^{3+}$ and $Mn^{2+}$-$Mn^{3+}$-$Mn^{4+}$ redox cycles play key roles in promoting the generation of ·OH. Therefore, Mn and Fe oxides on the catalyst surfaces have strong catalytic ozonation abilities.

### Catalytic ozonation performance of catalysts

Figure 2 shows the degradation and mineralization of phenol in adsorption, ozonation, and catalytic ozonation systems, as well as the changes in $O_3$ concentration in solution. The

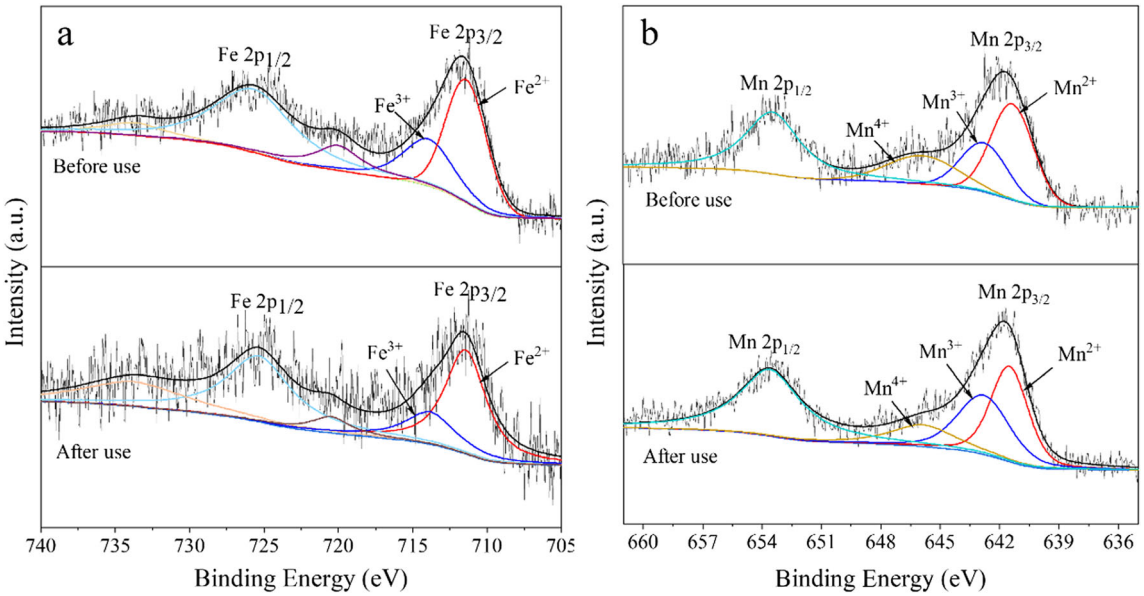


**Fig. 1** Fe2p (**a**) and Mn 2p (**b**) XPS spectra of the fresh and used Fe or Mn/GAC (0.10) catalysts

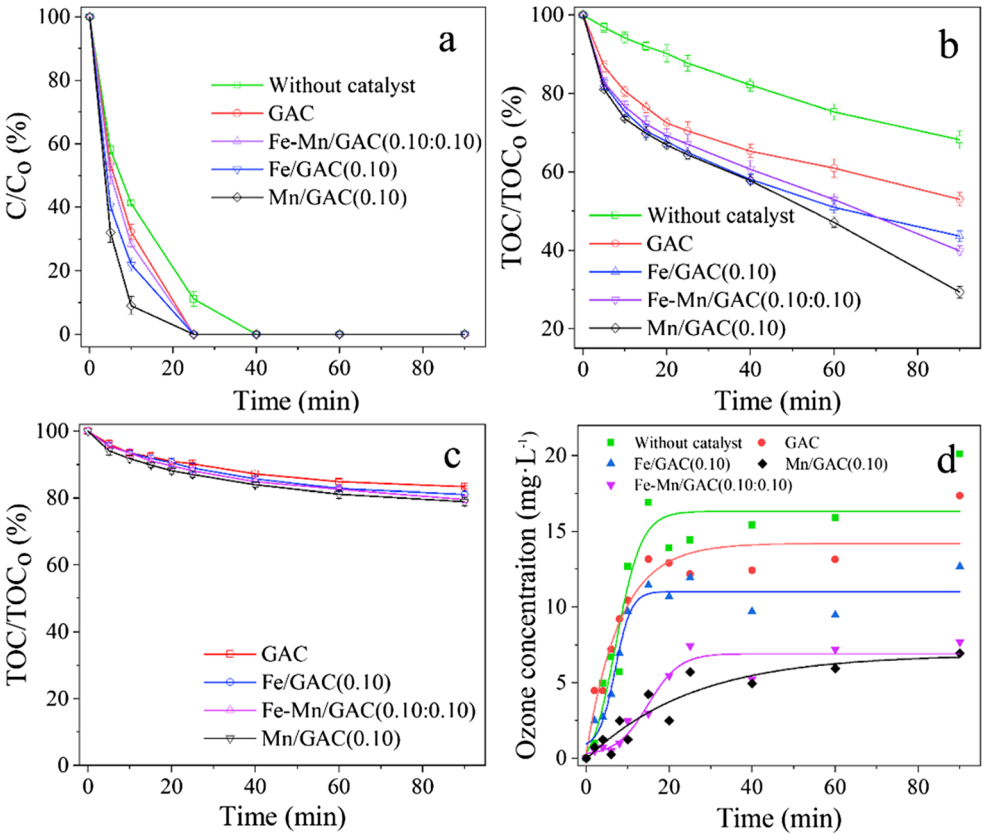


**Fig. 2** Removal of phenol (**a**) and TOC (**b**) in aqueous dispersions of various catalysts with $O_3$ ($C_{phenol}$ = 200.0 mg $L^{-1}$; catalysts dosage = 1.0 g $L^{-1}$; $O_3$ concentration = 22.0 mg $L^{-1}$). Removal of TOC for adsorption of various catalysts (**c**) ($C_{phenol}$ = 200.0 mg $L^{-1}$; catalysts dosage = 1.0 g $L^{-1}$). Residue ozone concentration in different systems (**d**) ($C_{phenol}$ = 200.0 mg $L^{-1}$; catalysts dosage = 1.0 g $L^{-1}$; $O_3$ concentration = 22.0 mg $L^{-1}$)

removal performances of phenol and TOC with respect to time under different experimental conditions were evaluated as shown in Fig. 2a and b, respectively. In Fig. 2a, ozonation alone removed 88.8% of phenol within 25 min, while phenol was completely eliminated in the first 25 min using GAC/$O_3$, Fe-Mn/GAC (0.10:0.10)/$O_3$, Fe/GAC (0.10)/$O_3$, and Mn/GAC (0.10)/$O_3$. $O_3$ was a powerful oxidant that reacted with organic compounds containing aromatic moieties and unsaturated bonds, which led to the rapid and complete removal of phenol (Zhu et al. 2017a). However, the catalytic ozonation systems using Fe and/or Mn/GACs had better phenol degradation performances than the GAC/$O_3$ system. This indicated that adding Fe and Mn improved the system's catalytic phenol ozonation ability.

As shown in Fig. 2b, only 31.8% of TOC was removed at a reaction time of 90 min when using $O_3$ alone. The degradation of phenol formed several intermediate products which were further converted to saturated compounds such as carboxylic acids, which could not be directly mineralized by $O_3$ (Ramseier and Gunten 2009). Consequently, the degree of mineralization of phenol using $O_3$ alone was not always satisfactory. For the GAC/$O_3$ system, the TOC removal efficiency reached 47.0% due to the adsorption and slight catalytic ability of GAC (Ma et al. 2004). The Fe/GAC (0.10)/$O_3$ and Fe-Mn/GAC (0.10:0.10)/$O_3$ showed higher activities than GAC/$O_3$, with TOC removal efficiencies of 56.4% and 60.1%, respectively. The Mn/GAC (0.10)/$O_3$ system had the highest degradation activity, and the TOC concentration in solution decreased by 70.7%. Obviously, adding Fe and/or Mn on the surface of the GAC significantly enhanced the TOC removal activity of the catalysts. It is generally believed that metal-supported catalysts can accelerate conversion of $O_3$ to ·OH free radicals and increase the $O_3$ utilization efficiency (Li et al. 2017). It is this behavior which gave Fe/GAC (0.10), Mn/GAC (0.10), and Fe-Mn/GAC (0.10:0.10) their excellent catalytic performances.

Since adsorption processes are very important for the mineralization of organic compounds during heterogenous catalytic ozonation, the TOC adsorption of different catalysts was investigated. As shown in Fig. 2c, 16.7%, 18.8%, 20.4%, and 21.0% of TOC were removed by the GAC, Fe/GAC (0.10), Fe-Mn/GAC (0.10:0.10), and Mn/GAC (0.10) systems, respectively, over a 90-min reaction. This demonstrates that the catalyst adsorption played an important role in the TOC removal process. Compared with the GAC adsorption process, the Fe and/or Mn/GACs showed no obvious increases in the TOC removal during adsorption due to low metal loadings. This suggests that the TOC removal in solution was mainly accomplished by oxidation.

The adsorption and ozonation experiments showed that the TOC removal efficiency of Fe and/or Mn/GAC/$O_3$ systems was higher compared with using adsorption or ozonation

alone. This suggests that significant interactions occur between the catalysts and $O_3$. To verify this hypothesis, different ozone concentrations were tested in different reaction systems, and the results are shown in Fig. 2d. The ozone concentration increased rapidly and then reached a dynamic equilibrium in all ozonation systems within the first 20 min. Moreover, the order of ozone equilibrium concentration was non-catalyst > GAC > Fe/GAC (0.10) > Fe-Mn/GAC (0.10:0.10) > Mn/GAC (0.10), which shows that adding catalysts significantly enhanced ozone decomposition. The order of ozone utilization efficiency was the same as the phenol mineralization efficiency order of the above five ozonation systems. Therefore, the catalytic performances of Fe and/or Mn/GACs were responsible for $O_3$ decomposition during ozonation. These results are similar to previous studies (Zhu et al. 2017a; Chen et al. 2018) which indicated that catalysts play important roles in mineralizing phenol.

## Effects of operating factors

The metal oxide loading affects not only the aggregation and dispersion of the catalyst, but also its crystallization and redox properties (Du et al. 2018). Therefore, the effect of Fe and/or Mn ion impregnation on phenol mineralization was evaluated, and the results are shown in Fig. 3. In a single Fe impregnation experiment, the removal efficiency of TOC showed a remarkable increase as the Fe concentration increased, reaching a maximum (56.4%) at an Fe impregnation concentration of 0.10 mol $L^{-1}$, and then began to decline. Interestingly, the single Mn impregnation experiment showed a similar trend, and a maximum TOC removal efficiency of 70.7% was obtained at a Mn impregnation concentration of 0.10 mol $L^{-1}$.

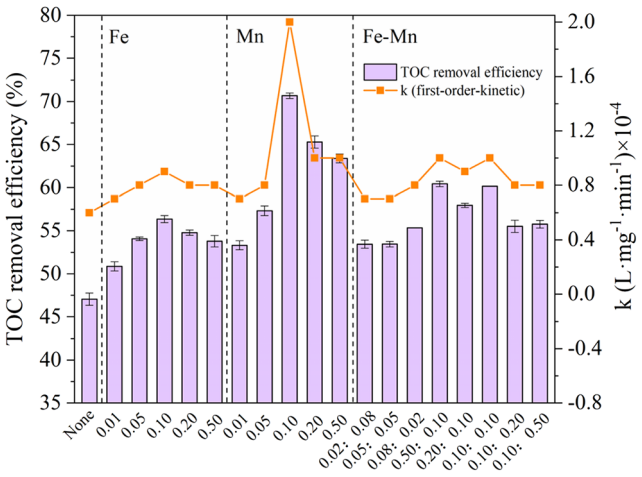


**Fig. 3** Effect of Fe or/and Mn impregnation concentrations on mineralization of phenol ($C_{phenol}$ = 200.0 mg $L^{-1}$; catalysts dosage = 1.0 g $L^{-1}$; ozone concentration = 22.0 mg $L^{-1}$)

Virgin GAC cannot provide enough active sites to catalyze the ozonation of phenol. However, the active sites of Fe or Mn/GACs increased as the Fe and Mn ion impregnation concentration increased, which enhanced the phenol mineralization capacities (He et al. 2010; Chen et al. 2018). On the other hand, overloading the GAC surface with Fe and Mn may block pores and decrease the total pore volume, specific surface area, and mean pore diameter of the catalysts, which would decrease the catalyst active sites (Li et al. 2009). Consistent with the above results, Dai et al. (2014) found that excess Ce loading decreased the catalytic ozonation performance of p-TSA by Ce/AC due to a decrease in the pore volume, special surface area, and pore diameter of the catalyst.

To investigate the catalytic properties of catalysts with Fe-Mn composite metal oxides, the efficiency of phenol mineralization was assessed using catalysts with different Fe-Mn impregnation ratios. As shown in Fig. 3, TOC removal by Fe-Mn/GAC (0.50:0.10) and Fe-Mn/GAC (0.10:0.10) was higher than that of other ratios, but far lower than that of Mn/GAC (0.10). These results show that 0.10 mol $L^{-1}$ was the threshold for inhibiting the catalytic ozonation performance of Fe or Mn/GAC. Therefore, there was a decrease in the number of active sites in Fe-Mn/GAC (0.10:0.10) due to pore blockage, which reduced the catalytic performance. In addition, it was found that the mineralization of phenol followed a first-order kinetic model in the Fe and/or Mn/GAC system, as shown in Fig. 3. The rate constant order of these ozonation systems was identical to the order of phenol mineralization efficiency. Moreover, the rate constant reached a maximum (2.0 L $mg^{-1}$ $min^{-1}$) at a Mn impregnation concentration of 0.10 mol $L^{-1}$, indicating that it had superior catalytic performance.

To investigate the roles of ·OH in ozonation alone and catalytic ozonation systems, respectively, TBA was selected as a scavenger, because of its high reaction rate constant of $6 \times 10^8$ $M^{-1}$ $s^{-1}$ with ·OH and only $3 \times 10^{-3}$ $M^{-1}$ $s^{-1}$ with ozone (Buxton et al. 1988). Figure 4a shows that the phenol removal efficiency reaches 100% in the catalytic ozonation system and 85.7% in ozonation alone system within the first 40 min. However, when TBA was added, the phenol removal efficiency decreased by 20.0% and 10.7% in the catalytic ozonation system with Mn/GAC (0.10) and ozonation alone at 40 min, respectively. Compared to the ozonation alone, a 9.3% decrease was obtained in the catalytic ozonation system in the presence of TBA, suggesting that catalytic ozonation by Mn/GAC (0.10) generated more ·OH.

It is well known that carbonate and bicarbonate are ozone decomposition inhibitors by scavenging ·OH without generating $O_2^-$ or other free radicals that can accelerate ozone decomposition (Staehelin and Hoigné 1985). Thus, the effect of carbonate on phenol mineralization was investigated by adding 250 mg $L^{-1}$ and 500 mg $L^{-1}$ $Na_2CO_3$ to the substrate solution.

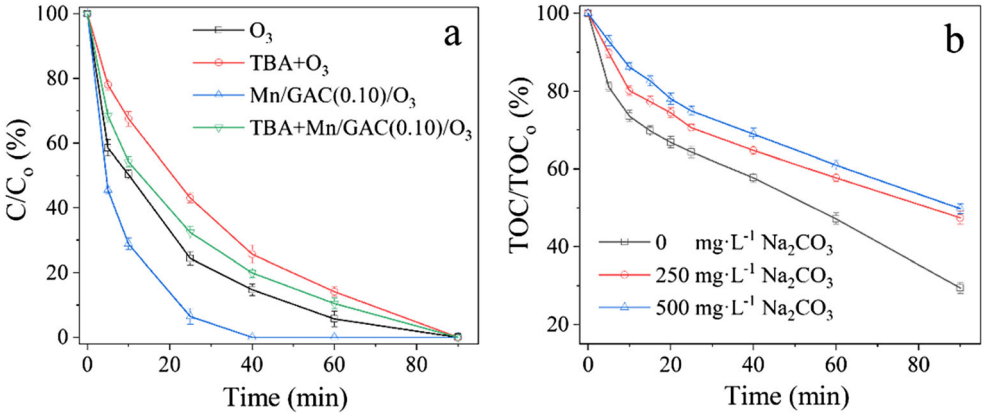


**Fig. 4** Effect of TBA in phenol catalytic ozonation process (**a**) ($C_{phenol}$ = 200.0 mg $L^{-1}$; Mn/GAC (0.10) dosage = 1.0 g $L^{-1}$; ozone concentration = 11.18 mg $L^{-1}$; TBA = 1.0 g $L^{-1}$). TOC removal in the presence of carbonate ions (**b**) ($C_{phenol}$ = 200.0 mg $L^{-1}$; Mn/GAC (0.10) dosage = 1.0 g $L^{-1}$; ozone concentration = 22.0 mg $L^{-1}$)

As depicted in Fig. 4b, the phenol mineralization was significantly affected after 250 mg $L^{-1}$ $Na_2CO_3$ was added, and the removal efficiency of TOC decreased by 18.1%. Further increasing the concentration of $Na_2CO_3$ to 500 mg $L^{-1}$ did not significantly inhibit phenol mineralization. The reactions between ·OH and $CO_3^{2-}$/$HCO_3^-$ can be described using Eqs. (1) and (2) (Buxton et al. 1988):

$$HCO_3^- + \cdot OH \rightarrow HCO_3^{\cdot -} + OH^- \quad k = 8.5 \times 10^6 M^{-1} s^{-1} \quad (1)$$

$$CO_3^{2-} + \cdot OH \rightarrow CO_3^{\cdot -} + OH^- \quad k = 3.9 \times 10^8 M^{-1} s^{-1} \quad (2)$$

The result obtained from the above experiment indicated that carbonate significantly decreased the TOC removal efficiency, which further verified that ·OH played an important role in catalytic ozonation using Mn/GAC (0.10).

## Catalytical ozonation mechanism

### Identification of intermediate products and their degradation pathways

GC-MS and HPLC showed that many intermediate products formed during the catalytic ozonation process, as shown in Table S2. According to the formation of intermediate products during the phenol degradation, possible pathways were tentatively proposed and are depicted in Fig. 5. It can be seen that the phenol oxidation during catalytic ozonation proceeded initially through the hydroxylation of the aromatic ring to form catechol, hydroquinone, and resorcinol. The dihydroxybenzenes, such as catechol and hydroquinone, were in redox equilibrium with benzoquinones (Zazo et al. 2005). Dihydroxybenzenes were further oxidized via hydroxylation to form trihydroxybenzenes (benzenetriol) (Kermani et al. 2018). These were decomposed into muconic, succinic, maleic, and fumaric acids via benzene ring cleavage and were further decomposed into oxalic and acetic acids (Zazo et al. 2005; Ramseier and Gunten 2009; Dai et al. 2014). Finally, aliphatic products containing carbonyl and carboxyl groups were oxidized to $CO_2$ and $H_2O$. The above phenol degradation pathway was mainly ascribed to two types of oxidation in the Fe and/or Mn/GAC/$O_3$ systems. In one type, direct oxidation of ozone was extremely selective for unsaturated aromatic and aliphatic compounds as well as specific functional groups via Criegee mechanism (Criegee 1953; Turhan and Uzman 2008). In the other type, the indirect oxidation of ·OH played an important role in the cleavage of benzene rings and unsaturated bonds due to its non-selectivity and high oxidation ability.

### Exploration of the catalytic mechanism

During heterogeneous catalytic ozonation, ozone can be efficiently converted to free radicals through its interactions with a catalyst (Zhu et al. 2017b; Centurião et al. 2019). The TBA experiment showed that the presence of Mn/GAC (0.10) significantly promoted the generation of ·OH, which indicated that the catalyst accelerated the conversion of ozone into ·OH. To investigate how the interaction between ozone and catalyst affects the free radical generation mechanism, different amounts of dissolved ozone both with and without catalyst, as well as the results obtained from FTIR, XPS, EDS, and CV, were comprehensively analyzed.

Ozone and organic compounds can adsorb onto the surface of a catalyst and participate in catalytic ozonation reactions in heterogeneous catalytic oxidation systems (Bai et al. 2016; Zhu et al. 2017b). It has been reported that ozone molecules can form five-membered rings with oxygen-containing groups on the catalyst surface via hydrogen bonds and electrostatic forces. These molecules are then decomposed into free radicals (·OH) via electron transfer processes (Zhang and Ma 2008; Zhao et al. 2009a; Zhao et al. 2009b). The FTIR analysis (Fig. S3) indicated that the surface hydroxyl groups of GAC participated in the catalytic ozonation process. However, the addition of Fe or Mn oxides did not increase the hydroxyl group density on the surface, indicating that free radical generation was not dominated by the interactions

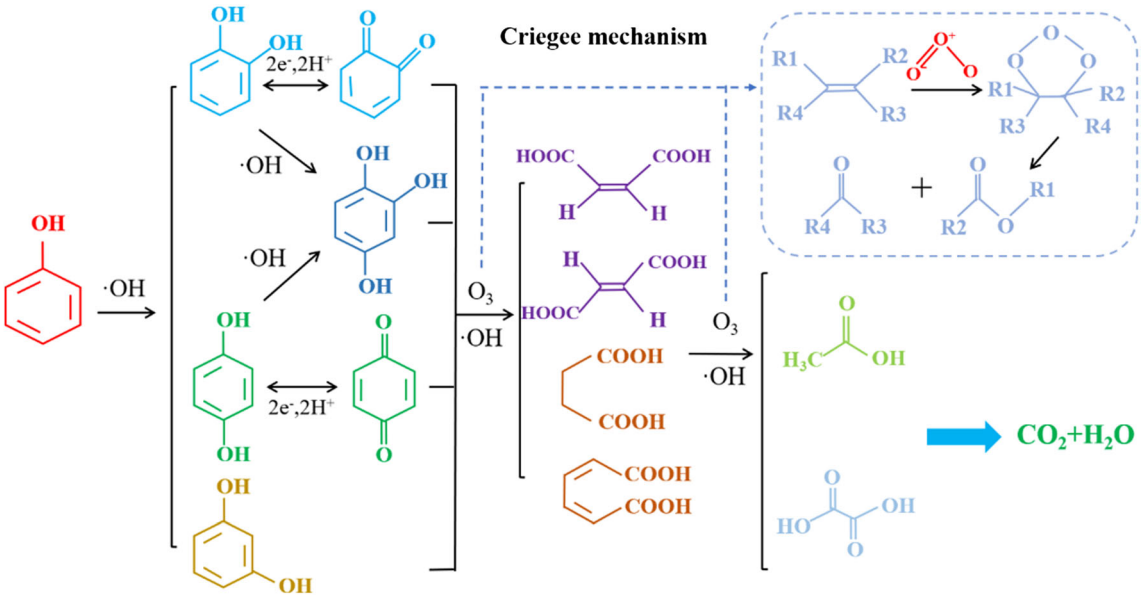


**Fig. 5** Proposed pathway of phenol degradation by catalytic ozonation ($C_{phenol}$ = 200.0 mg $L^{-1}$; catalysts dosage = 1.0 g $L^{-1}$; ozone concentration = 22.0 mg $L^{-1}$)

between ozone and hydroxyl groups on the surface of the catalyst. XPS analysis showed that the $Fe^{2+}$-$Fe^{3+}$ and $Mn^{2+}$-$Mn^{3+}$-$Mn^{4+}$ redox cycles were involved in the catalytic ozonation by Fe and/or Mn on GACs.

Previous studies showed that the recycling of $Fe^{2+}$-$Fe^{3+}$ and $Mn^{2+}$-$Mn^{3+}$-$Mn^{4+}$ played key roles in promoting the generation of ·OH (Lv et al. 2010; Bai et al. 2016). The response mechanisms of these redox couples can be represented by the following equations (Xing et al. 2011; Wang and Bai 2017):

$$\equiv M^{n+1} + O_3 \rightarrow \equiv M^{n+} + \cdot OH + HO_2^{\cdot} + O_2 \quad (3)$$

$$\equiv M^{n+} + O_3 + H^+ \rightarrow \equiv M^{n+1} + \cdot OH + O_2 \quad (4)$$

Besides, the electron process, through the redox recycling of $Fe^{2+}$-$Fe^{3+}$ and $Mn^{2+}$-$Mn^{3+}$-$Mn^{4+}$, is considered to be a significant process for catalytic ozonation (Lv et al. 2010). To further investigate the electron transfer process at the water-catalyst interface, the cyclic voltammetry behaviors of GAC and Fe and/or Mn/GAC electrodes were analyzed in a 3 wt% NaCl solution in an ozone atmosphere. Figure 6 shows that no significant redox current was observed on the GAC electrode, while both Fe- and/or Mn-modified electrodes showed obvious current signals. In addition, the order of the redox current was Mn/GAC (0.10) > Fe-Mn/GAC (0.10:0.10) > Fe/GAC (0.10), which is identical to the order of phenol mineralization efficiency. These results showed that both the strong interaction between catalyst and ozone and the enhanced interfacial electron transfer capability improved the catalytic activity of the modified catalysts. The above analyses show that the catalytic effects of Fe and/or Mn/GAC were mainly attributed to the recycling of $Fe^{2+}$-$Fe^{3+}$ and $Mn^{2+}$-$Mn^{3+}$-$Mn^{4+}$, and changes in the concentration of dissolved ozone further demonstrated that the catalyst enhanced ozone's ability to produce hydroxyl radicals.

However, compared with the Mn/GAC (0.10)/$O_3$ system, the Fe-Mn/GAC (0.10:0.10)/$O_3$ system exhibited poorer TOC removal performance. This is inconsistent with a previous study which showed that combining $FeO_x$ and $MnO_x$ led to a synergistic effect which improved catalytic ozonation (Tang et al. 2016). Some literatures have showed that magnetite and $MnO_2$ can form a galvanic corrosion coupling product, resulting in strong interactions on the catalyst surfaces, which cause Fe and Mn to simultaneously dissolve in neutral environments (Nakazawa et al. 2016; Saavedra et al. 2018). Fe and

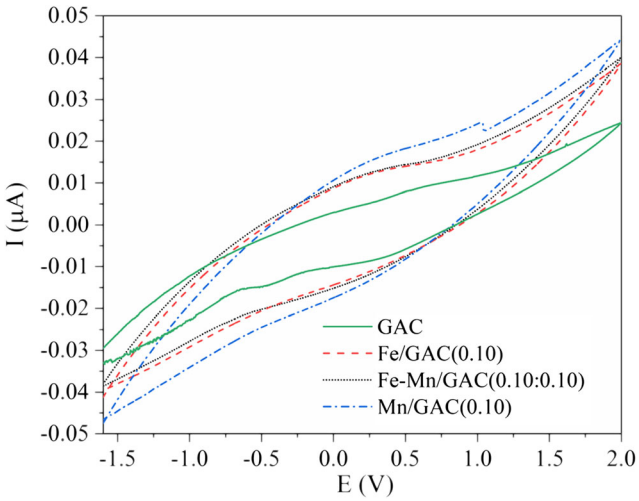


**Fig. 6** Cyclic voltammetry scans of GAC, Fe/GAC (0.10), Fe-Mn/GAC (0.10:0.10), and Mn/GAC (0.10) electrodes in 3 wt% NaCl solution with ozone (22.0 mg $L^{-1}$), Scan rate: 0.05 V $s^{-1}$

Mn can be released via galvanic interactions according to Eqs. (5) and (6):

$$3Fe_3O_4 \rightarrow 4\ (Fe_2O_3 \text{ or } FeOOH) + Fe^{2+} + 2e^- \quad (5)$$

$$MnO_2 + 4H^+ + 2e^- \rightarrow Mn^{2+} + 2H_2O \quad (6)$$

XPS analysis indicated that magnetite ($Fe_3O_4$) and $MnO_2$ were present on the surface of Fe-Mn/GAC, and carboxylic acids formed during the reaction process rapidly reduced the solution pH (Fig. S4). In addition, Nakazawa et al. (2016) showed that carbon materials could enhance galvanic corrosion by improving the conductivity between cathode and anode. Analysis of leaching metal ions (Table S4) showed that the concentrations of Fe and Mn ions in solution from the Fe-Mn/GAC (0.10:0.10)/$O_3$ system were significantly higher compared with those of the Fe/GAC (0.10)/$O_3$ and Mn/GAC (0.10)/$O_3$ systems. This confirmed the above inference about the presence of galvanic corrosion on the Fe-Mn/GAC surface. Therefore, the poor catalytic performance of Fe-Mn/GAC (0.10:0.10) is attributed to the reduction in the number of active sites, which occurred mainly due to the galvanic corrosion of $Fe_3O_4$ and $MnO_2$ which formed dissolved $Fe^{2+}$ and $Mn^{2+}$, respectively.

Therefore, in heterogeneous catalytic ozonation systems, the mineralization of organic compounds can be divided into two general reaction pathways: direct reactions with ozone and indirect reactions with free radicals generated from interactions between ozone and catalysts. Based on the above analyses, possible catalytic mechanisms of Fe and/or Mn/GAC are tentatively proposed and shown in Fig. 7.

## The stability of catalysts

Since industrial applications require catalysts to remain active over a long period of time, the reusability of the prepared catalysts in the catalytic ozonation of phenol wastewater was examined. Figure 8a shows that no remarkable changes were observed in the catalytic performance of the prepared catalysts after the fifth run, and the TOC removal efficiencies was only decreased by 7.2% (Fe/GAC (0.10)) and 9.5% (Mn/GAC (0.10)). This indicated that both Fe/GAC (0.10) and Mn/GAC (0.10) were stable during continuous catalytic ozonation. However, the TOC removal efficiency decreased by 14.7% after the fifth run, which can be ascribed to fewer active catalytic sites due to galvanic corrosion on the surface of Fe-Mn/GAC (0.10:0.10). The leaching of Fe and Mn from Fe and/or Mn/GAC catalysts during catalytic ozonation was investigated using ICP-OES, as shown in Table S4. Based on the results, at a reaction time of 90 min, the concentrations of Fe and Mn in aqueous solution using the Fe/GAC (0.10)/$O_3$ and Mn/GAC (0.10)/$O_3$ systems were 0.06 mg $L^{-1}$ and 0.07 mg $L^{-1}$, respectively, which implies that Fe and Mn were stable on the catalysts. Fe (0.36 mg $L^{-1}$) and Mn (0.45 mg $L^{-1}$) were more likely to be released from the surface of Fe-Mn/GAC (0.10:0.10) compared with the Fe or Mn/GAC

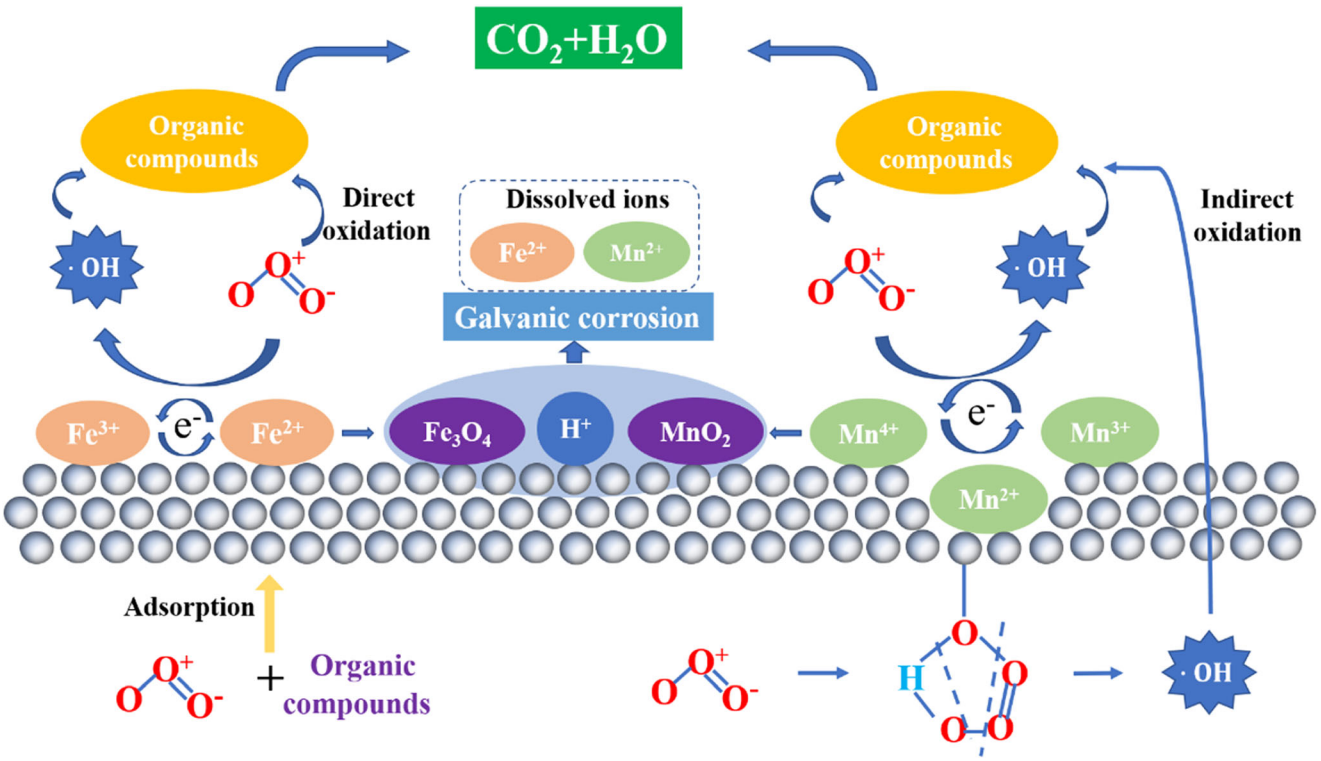


**Fig. 7** Proposed mineralization mechanism of phenol in Fe or/and Mn/GAC catalytic ozonation systems

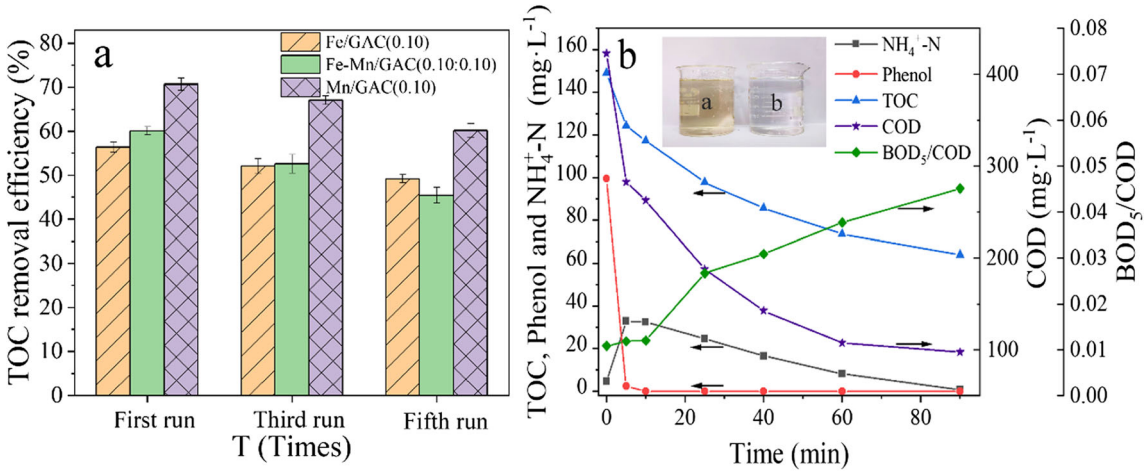


**Fig. 8** Catalytic performance of catalysts in successive ozonation runs (**a**) ($C_{phenol}$ = 200.0 mg $L^{-1}$; catalysts dosage = 1.0 g $L^{-1}$; ozone concentration = 22.0 mg $L^{-1}$; Each run time = 90 min); phenol, TOC, and COD removal and the evolution of $NH_4^+$-N and biodegradability index during catalytic ozonation (**b**); inset: color change of water sample before (**a**) and after (**b**) reaction (Mn/GAC (0.10) catalysts dosage = 1.0 g $L^{-1}$; ozone concentration = 22.0 mg $L^{-1}$)

(0.10) catalysts, which is attributed to the galvanic corrosion of the Fe-Mn/GAC surface.

## Application to secondary petrochemical effluent

To verify the performance of the catalytic ozonation system using actual wastewater, ozonation was used to treat secondary petrochemical effluent with Mn/GAC (0.10). As shown in Fig. 8b, when the phenol removal efficiency was 100%, the TOC decreased from 148.9 to 63.9 mg $L^{-1}$ with a mineralization efficiency of 57.1%, and the COD decreased from 422.5 to 97.5 mg $L^{-1}$ with a removal efficiency of 76.9%. The B/C increased from 0.011 to 0.045 after 90 min of catalytic ozonation, indicating the biochemical properties of the treated effluent were significantly improved. In addition, the $NH_4^+$-N concentration increased to 33.0 mg $L^{-1}$ in the first 5 min, suggesting that some nitrogen–containing derivatives were produced during the catalytic ozonation of secondary petrochemical effluent. Afterwards, the $NH_4^+$-N concentration decreased to 0.8 mg $L^{-1}$, which was attributed to indirect oxidation by ·OH and adsorption by the Mn/GAC (0.10) catalyst (Chen et al. 2017b; Kuang et al. 2018). In addition, it was found that the Mn/GAC (0.10) catalytic ozonation system significantly decolorized the secondary petrochemical effluent which was originally a transparent yellow liquid. The ecotoxicity evolution results in Fig. S5 show a slight toxicity increase in the first 5 min, which is possibly due to the generation of additional bio-inhibitory compounds during the degradation of phenol (Zhu et al. 2017b). However, the luminous intensity of Vibrio fischeri increased from ~ 450 to ~840 mV at 90 min of the catalytic ozonation process, suggesting that the process significantly decreased the toxicity of the secondary petrochemical effluent. In summary, catalytic ozonation based on Mn/GAC (0.10) notably improved the water quality index of secondary petrochemical effluent and efficiently treated secondary petrochemical effluent.

## Engineering significance

The findings of this study have demonstrated that the Mn/GAC (0.10)/$O_3$ catalyst is a stable and high-performance material for mineralizing phenol-containing wastewater. Due to this high efficiency, low cost, and simple operation of the catalyst, it can also be used for other refractory organic wastewaters. Due to the proper particle size of the catalyst (18–40 mesh), separation and recovery of the catalyst in heterogeneous catalytic ozonation was not an issue. The Mn/GAC (0.10)/$O_3$ catalyst effectively treated secondary petrochemical effluent, and the results of this study improve the understanding of catalytic ozonation when used to treat secondary petrochemical effluent. In addition, this study also found that galvanic corrosion occurred in the Fe-Mn/GAC-based catalytic ozonation system in an acidic environment. This may provide a good starting point for further application and development of bimetallic catalysts in catalytic ozonation.

## Conclusions

Fe and/or Mn/GAC catalysts were successfully prepared by precipitation-calcination and used for the treatment of phenol-containing wastewater. The catalytic performance order of the catalysts was Mn/GAC (0.10) > Fe-Mn/GAC (0.10:0.10) > Fe/GAC (0.10), and the Mn/GAC (0.10)/$O_3$ system removed approximately 23.7% more TOC compared with the GAC/$O_3$ system. Fe and/or Mn/GACs significantly enhanced the decomposition of $O_3$ into ·OH, which played an important role in phenol mineralization. Some intermediate products of

phenol degradation were identified, and a possible degradation pathway was proposed. The results of XPS, CV, and other experiments indicated that introducing Fe and Mn enhanced the interfacial electron transfer through $Fe^{2+}$-$Fe^{3+}$ and $Mn^{2+}$-$Mn^{3+}$-$Mn^{4+}$ redox cycles, which increased the catalytic activity. Galvanic corrosion occurred between $Fe_3O_4$ and $MnO_2$ on the surface of the Fe-Mn/GAC, which decreased its catalytic activity. Fe and Mn/GACs (0.10) still had high catalytic activities after 5 cycles, indicating that they were promising catalysts for the treatment of phenol-containing wastewater. The Mn/GAC/$O_3$ system significantly improved the quality of actual secondary petrochemical effluent, including reducing the COD, TOC, $NH_4^+$-N, water color, and ecotoxicity, thus demonstrating that it had great potential in practical engineering applications. This study provides a new insight for the treatment of phenol-containing wastewater and secondary petrochemical effluent by catalytic ozonation.

**Funding** The authors received financial support from the National Natural Science Foundation of China (NSFC) (No. 21876159) and the Fundamental Research Funds for the Central Universities (No. 2652018181; No. 2652018202).

## References

Afzal S, Quan X, Chen S, Wang J, Muhammad D (2016) Synthesis of manganese incorporated hierarchical mesoporous silica nanosphere with fibrous morphology by facile one-pot approach for efficient catalytic ozonation. J Hazard Mater 318:308–318

Álvarez PM, Pocostales JP, Beltrán FJ (2011) Granular activated carbon promoted ozonation of a food-processing secondary effluent. J Hazard Mater 185:776–783

Bai ZY, Yang Q, Wang JL (2016) Catalytic ozonation of sulfamethazine using Ce0.1Fe0.9OOH as catalyst: mineralization and catalytic mechanisms. Chem Eng J 300:169–176

Buxton GV, Greenstock CL, Helman WP, Ross WP (1988) Critical review of rate constants for reactions of hydrated electrons, hydrogen atoms and hydroxyl radicals in aqueous solution. J Phys Chem Ref Data 17:513–886

Centurião APSL, Balsissarelli VZ, Scaratti G, de Amorim SM, Moreira RFPM (2019) Enhanced ozonation degradation of petroleum refinery wastewater in the presence of oxide nanocatalysts. Environ Technol 40:1239–1249

Chen CM, Wei LY, Guo X, Guo SH, Yan GX (2014a) Investigation of heavy oil refinery wastewater treatment by integrated ozone and activated carbon-supported manganese oxides. Fuel Process Technol 124:165–173

Chen CM, Chen HS, Guo X, Guo SH, Yan GX (2014b) Advanced ozone treatment of heavy oil refining wastewater by activated carbon supported iron oxide. J Ind Eng Chem 20:2782–2791

Chen CM, Li Y, Ma WF, Guo SH, Wang QH, Li QX (2017a) Mn-Fe-Mg-Ce loaded $Al_2O_3$ catalyzed ozonation for mineralization of refractory organic chemicals in petroleum refinery wastewater. Sep Purif Technol 183:1–10

Chen JF, Liu SN, Yan J, Wen JJ, Hu YY, Zhang WW (2017b) Intensive removal efficiency and mechanisms of carbon and ammonium in municipal wastewater treatment plant tail water by ozone oyster shells fix-bed bioreactor-membrane bioreactor combined system. Ecol Eng 101:75–83

Chen WR, Li XK, Tang YM, Zhou JL, Wu D, Wu Y, Li LS (2018) Mechanism insight of pollutant degradation and bromate inhibition by Fe-Cu-MCM-41 catalyzed ozonation. J Hazard Mater 346:226–233

Cheng XX, Liang H, Qu FS, Ding A, Chang HQ, Liu B, Tang XB, Wu DJ, Li GB (2017) Fabrication of Mn oxide incorporated ceramic membranes for membrane fouling control and enhanced catalytic ozonation of *p*-chloronitrobenzene. Chem Eng J 308:1010–1020

Chinese State Environment Protection Bureau (CSEPB) (2002) Water and wastewater monitoring analysis methods. Chinese Environment Science Press, Beijing, pp 210–276

Criegee R (1953) Uber den verlauf der ozonspaltung 0.3. Justus Liebigs Ann Chem 583:1–2

Dai QZ, Wang JY, Chen J, Chen JM (2014) Ozonation catalyzed by cerium supported on activated carbon for the degradation of typical pharmaceutical wastewater. Sep Purif Technol 127:112–120

Du XY, Li CT, Zhao LK, Zhang J, Gao L, Sheng JJ, Yi YY, Chen JQ, Zeng GM (2018) Promotional removal of HCHO from simulated flue gas over Mn-Fe oxides modified activated coke. Appl Catal B Environ 232:37–48

Edwards-Brandt J, Shorney-Darby H, Neemann J, Hesby J, Tona C (2007) Use of ozone for disinfection and taste and odor control at proposed membrane facility. Ozone Sci Eng 29:281–286

Faria PCC, Monteiro DCM, Órfão JJM, Pereira MFR (2009) Cerium, manganese and cobalt oxides as catalysts for the ozonation of selected organic compounds. Chemosphere 74:818–824

Gümüş D, Akbal F (2017) A comparative study of ozonation, iron coated zeolite catalyzed ozonation and granular activated carbon catalyzed ozonation of humic. Chemosphere 174:218–231

He ZQ, Zhang AL, Song S, Liu ZW, Chen JM, Xu XH, Liu WP (2010) $\gamma$-$Al_2O_3$ modified with praseodymium: an application in the heterogeneous catalytic ozonation of succinic acid in aqueous solution. Ind Eng Chem Res 49:12345–12351

Huang YX, Cui CC, Zhang DF, Li L, Pan D (2015) Heterogeneous catalytic ozonation of dibutyl phthalate in aqueous solution in the presence of iron-loaded activated carbon. Chemosphere 119:295–301

Kermani M, Kakavandi B, Farzadkia M, Esrafili A, Jokandan SF, Shahsavani A (2018) Catalytic ozonation of high concentrations of catechol over $TiO_2$@$Fe_3O_4$ magnetic core-shell nanocatalyst: optimization, toxicity and degradation pathway studies. J Clean Prod 192:597–607

Kuang PJ, Chen N, Feng CP, Li M, Dong SS, Lv L, Zhang J, Hu ZX, Deng Y (2018) Construction and optimization of an iron particle-zeolite parking electrochemical-adsorption system for the simultaneous removal of nitrate and by-products. J Taiwan Inst Chem Eng 86:101–112

Li LS, Ye WY, Zhang QY, Sun FQ, Lu P, Li XK (2009) Catalytic ozonation of dimethyl phthalate over cerium supported on activated carbon. J Hazard Mater 170:411–416

Li JR, Chen JS, Yu YK, He C (2015) Fe-Mn-Ce/ceramic powder composite catalyst for highly volatile elemental mercury removal in simulated coal-fired flue gas. J Ind Eng Chem 25:352–358

Li CH, Jiang F, Sun DZ, Qiu B (2017) Catalytic ozonation for advanced treatment of incineration leachate using ($MnO_2$-$Co_3O_4$)/AC as a catalyst. Chem Eng J 325:624–631

Li QS, Yu JW, Chen WZ, Ma XY, Li GX, Chen GY, Deng J (2018) Degradation of triclosan by chlorine dioxide: reaction mechanism, 2,4-dichlorophenol accumulation and toxicity evaluation. Chemosphere 207:449–456

Liang XL, Liu P, He HP, Wei GL, Chen TH, Tan W, Tan FD, Zhu JX, Zhu RL (2016) The variation of cationic microstructure in Mn-doped

spinel ferrite during calcination and its effect in formaldehyde catalytic oxidation. J Hazard Mater 306:305–312

Liu P, He HP, Wei GL, Liang XL, Qi FH, Tan W, Zhu JX, Zhu RL (2016) Effect of Mn substitution on the promoted formaldehyde oxidation over spinel ferrite: catalyst characterization, performance and reaction mechanism. Appl Catal B Environ 182:476–484

Lv AH, Hu C, Nie YL, Qu JH (2010) Catalytic ozonation of toxic pollutants over magnetic cobalt and manganese co-doped $\gamma$-$Fe_2O_3$. Appl Catal B Environ 100:62–67

Ma J, Sui MH, Chen ZL, Wang LN (2004) Degradation of refractory organic pollutants by catalytic ozonation-activated carbon and Mn-loaded activated carbon as catalysts. Ozone Sic Eng 26:3–10

Ma ZC, Zhu L, Lu XY, Xing ST, Wu YS, Gao YZ (2014) Catalytic ozonation of *p*-nitrophenol over mesoporous Mn-Co-Fe oxide. Sep Purif Technol 133:357–364

Ma DH, Chen LJ, Wu YC, Liu R (2016) Evaluation of the removal of antiestrogens and antiandrogens via ozone and granular activated carbon using bioassay and fluorescent. Chemosphere 153:346–355

Massa A, Hernández S, Ansaloni S, Castellino M, Russo N, Fino D (2018) Enhanced electrochemical oxidation of phenol over manganese oxides under mild wet air oxidation conditions. Electrochim Acta 273:53–62

Nakazawa H, Nakamura S, Odashima S, Hareyama W (2016) Effect of carbon black to facilitate galvanic leaching of copper from chalcopyrite in the presence of manganese (IV) oxide. Hydrometallurgy 163:69–76

Nawrocki J, Kasprzyk-Hordern B (2010) The efficiency and mechanism of catalytic ozonation. Appl Catal B Environ 99:27–42

Qi F, Xu BB, Zhao L, Chen ZG, Zhang LQ, Sun DZ, Ma J (2012) Comparison of the efficiency and mechanism of catalytic ozonation of 2, 4, 6-trichloroanisole by iron and manganese modified bauxite. Appl Catal B Environ 121-122:171–181

Ramseier MK, Gunten UV (2009) Mechanisms of phenol ozonation—kinetics of formation of primary and secondary reaction products. Ozone Sic Eng 31:201–205

Rivera Utrilla J, Sánchez Polo M, Gómez Serrano V, Álvarez PM, Alvim Ferraz MCM, Dias JM (2011) Activated carbon modifications to enhance its water treatment applications. An overview. J Hazard Mater 187:1–23

Saavedra A, García-Meza JV, Cortón E, González I (2018) Understanding galvanic interactions between chalcopyrite and magnetite in acid medium to improve copper (bio) leaching. Electrochim Acta 265:569–576

Staehelin J, Hoigné J (1985) Decomposition of ozone in water in the presence of organic solutes acting as promoters and inhibitors of radical chain reactions. Environ Sci Technol 19:1206–1213

Strohmeier BR, Hercules DM (1984) Surface spectroscopic characterization of manganese/aluminum oxide catalysts. J Phys Chem 88: 4922–4929

Tan CQ, Gao NY, Deng Y, Deng J, Zhou SQ, Li J, Xin XY (2014) Radical induced degradation of acetaminophen with $Fe_3O_4$ magnetic nanoparticles as heterogeneous activator of peroxymonosulfate. J Hazard Mater 276:452–460

Tang SF, Yuan DL, Zhang Q, Liu YM, Liu ZQ, Huang HM (2016) Fe-Mn bi-metallic oxides loaded on granular activated carbon to enhance dye removal by catalytic ozonation. Environ Sci Pollut Res 23: 18800–18808

Turhan K, Uzman S (2008) Removal of phenol from water using ozone. Desalination 229:257–263

Umezawa Y, Reilley CN (1978) Effect of argon ion bombardment on metal complexes and oxides studied by x-ray photoelectron spectroscopy. Anal Chem 50:1290–1295

Vaiano V, Matarangolo M, Murcia JJ, Rojas H, Navío JA, Hidalgo MC (2018) Enhanced photocatalytic removal of phenol from aqueous solutions using ZnO modified with Ag. Appl Catal B Environ 225:197–206

Wang JL, Bai ZY (2017) Fe-based catalysts for heterogeneous catalytic ozonation of emerging contaminants in water and wastewater. Chem Eng J 312:79–98

Wang H, Jing MM, Wu Y, Chen WL, Ran Y (2018) Effective degradation of phenol via Fenton reaction over CuNiFe layered double hydroxides. J Hazard Mater 353:53–61

Wu CH, Kuo CY, Chang CL (2008) Homoheneous catalytic ozonation of C.I. reactive red 2 by metallic ions in a bubble column reactor. J Hazard Mater 154:748–755

Xing ST, Zhou ZC, Ma ZC, Wu YS (2011) Characterization and reactivity of $Fe_3O_4$/$FeMnO_x$ core/shell nanoparticles for methylene blue discoloration with $H_2O_2$. Appl Catal B Environ 107:386–392

Zazo JA, Casas JA, Mohedano AF, Gilarranz MA, Rodríguez JJ (2005) Chemical pathway and kinetics of phenol oxidation by Fenton's reagent. Environ Sci Technol 39:9295–9302

Zeng ZQ, Zou HK, Li X, Arowo M, Sun BC, Chen JF, Chu GW, Shao L (2013) Drgradation of phenol by ozone in the presence of Fenton reagent in a rotating packed bed. Chem Eng J 229:404–411

Zhang T, Ma J (2008) Catalytic ozonation of trace nitrobenzene in water with synthetic goethite. J Mol Catal A Chem 279:82–89

Zhang ZF, Liu BS, Wang F, Zheng S (2015) High-temperature desulfurization of hot coal gas on Mo modified Mn/KIT-1 sorbents. Chen Eng J 272:69–78

Zhao L, Ma J, Sun ZZ, Liu HL (2009a) Mechanism of heterogeneous catalytic ozonation of nitrobenzene in aqueous solution with modified ceramic honeycomb. Appl Catal B Environ 89:326–334

Zhao L, Sun Z, Ma J (2009b) Novel relationship between hydroxyl radical initiation and surface group of ceramic honeycomb supported metals for the catalytic ozonation of nitrobenzene in aqueous solution. Environ Sci Technol 4:4157–4163

Zhao H, Dong YM, Wang GL, Jiang PP, Zhang JJ, Wu LN, Li K (2013) Novel magnetically separable nanomaterials for heterogeneous catalytic ozonation of phenol pollutant: NiFe2O4 and their performances. Chem Eng J 219:295–302

Zhu SM, Dong BZ, Yu YH, Bu LJ, Deng J, Zhou SQ (2017a) Heterogeneous catalysis of ozone using ordered mesoporous $Fe_3O_4$ for degradation of atrazine. Chen Eng J 328:527–535

Zhu H, Ma WC, Han HG, Han YX, Ma WW (2017b) Catalytic ozonation of quinoline using nano-MgO: efficacy, pathways, mechanisms and its application to real biologically pretreated coal gasification wastewater. Chen Eng J 327:91–99